NASA Technical Memorandum 79152

FEASIBILITY OF DETERMINING FLAT ROOF HEAT LOSSES USING AERIAL THERMOGRAPHY

Robert L. Bowman and John R. Jack
Lewis Research Center
Cleveland, Ohio

Prepared for the
Thirteenth International Symposium on Remote Sensing
of Environment
sponsored by the University of Michigan
Ann Arbor, Michigan, April 23-27, 1979

FEASIBILITY OF DETERMINING FLAT ROOF HEAT LOSSES USING AERIAL THERMOGRAPHY

Robert L. Bowman and John R. Jack
NASA Lewis Research Center
Cleveland, Ohio

ABSTRACT

The utility of aerial thermography for determining rooftop heat losses was investigated experimentally using several completely instrumented test roofs with known thermal resistances. Actual rooftop heat losses were obtained both from in-situ instrumentation and aerial thermography obtained from overflights at an altitude of 305 m. In general, the remotely determined roof surface temperatures agreed very well with those obtained from ground measurements. The roof heat losses calculated using the remotely determined roof temperature agreed to within 17% of those calculated from $1/R\ \Delta T$ using ground measurements. However, this agreement may be fortuitous since the convective component of the heat loss is sensitive to small changes in roof temperature and to the average heat transfer coefficient used, whereas the radiative component is less sensitive. Thus, at this time, it is felt that an acceptable quantitative determination of roof heat losses using aerial thermography is only feasible when the convective term is accurately known or minimized. The sensitivity of the heat loss determination to environmental conditions was also evaluated. The analysis showed that the most reliable quantitative heat loss determinations can probably be obtained from aerial thermography taken under conditions of total cloud cover with low wind speeds and at low ambient temperatures.

E-9981

INTRODUCTION

NASA has been engaged for some years in an energy conservation program due to reduced energy resources and increased energy costs. As a part of this program, aerial thermographs of all the NASA field centers (ref. 1) were obtained to detect and identify areas of large energy loss. The resulting infrared imagery was very successful in locating areas of excessive energy losses so that corrective action could be taken. The cost benefits resulting from the thermographic surveys were substantial and impressive. Private sector users of aerial thermography have also achieved very impressive results in locating areas of energy loss.

The utility of aerial thermography for energy conservation in the industrial and commercial sector could be increased if quantitative heat losses from rooftops could be determined from analytical models using the remote data. With such information, a building owner could determine the cost benefits to be achieved by renovating his roof. In addition, roof repairs could be prioritized based upon the amount of energy being lost. Thus, a program to determine the feasibility of determining quantitative heat losses from industrial and commercial type rooftops was initiated by NASA with the participation of the General Services Administration (GSA) at the Denver Federal Center. The GSA was involved because of the large number of commercial/industrial type government buildings under their jurisdiction.

Several completely instrumented test sites on roofs of structures with known thermal resistances were overflown at an altitude of 305 m (1000 ft) with a 0.76-m (2.5-ft) resolution element to obtain calibrated thermal data in the 8 to 14 μm wavelength band. Actual rooftop heat losses were ther calculated from the remotely sensed temperature data using a generally accepted flat roof heat transfer model.

This paper presents a summary of the preliminary results obtained using the heat transfer model and a discussion of the effects of environmental parameters such as wind speed, ambient temperature, and sky radiation on the determination of roof surface temperatures and quantitative heat losses using aerial thermography.

HEAT TRANSFER ANALYSIS

Only the heat transfer processes between a flat roof surface and the environment will be considered in this paper. A model for an isolated flat horizontal roof was chosen because its radiation view factor is zero for all sources of radiation other than the sky, and is also the simplest physical model for convective heat transfer. If it is not feasible to determine quantitative heat loss remotely for this case, then it will not be feasible to do so in the more complicated case where extraneous radiation sources and sloped roofs are encountered. In addition, the flat roof is the typical roof used on industrial and commercial structures.

The heat transfer processes for such a roof are shown figure 1. The net heat flux, Q, is given by

Q = radiation emitted by the roof - radiation absorbed by the roof from the surroundings + convection between the roof and the outside air

$$Q = q_\varepsilon - q_\alpha + q_c$$

The radiation emitted by the roof is given by

$$q_\varepsilon = \varepsilon\sigma T_R^4 \qquad (W/m^2) \tag{1}$$

where

T_R roof surface temperature (K)

ε roof surface emittance

σ Stephan-Boltzmann constant = 5.67×10^{-8} W/m^2 $(K)^4$

= 1.71×10^{-9} Btu/hr-ft^2 $(^\circ R)^4$

Of the radiation incident on the roof, the fraction absorbed by the roof is

$$q_\alpha = \alpha q_s = \varepsilon q_s \qquad (W/m^2) \tag{2}$$

where

α roof absorptance which is equal to ε for a gray body surface

q_s total radiant flux (calorimetric) at all wavelengths from the surroundings such as the sky, trees, and nearby buildings

For this analysis, since the roof is considered isolated, q_s will be from the sky only and is dependent on the ambient air temperature, the extent of cloud cover, and their altitude (see refs. 2 and 3). The total sky radiation has been described in terms of a calorimetric sky temperature, T_s (ref. 2), such that

$$T_s = \left(\frac{q_s}{\sigma}\right)^{1/4} \tag{3}$$

In this equation, T_s is the temperature of a blackbody that radiates the same total flux as the sky. On a night with zero cloud cover, T_s is considerably less than the ambient air temperature T_A, while for total cloud cover, T_s is assumed equal to T_A (refs. 2 and 3).

The convective heat flux is given by:

$$q_c = h_c(T_R - T_A) \tag{4}$$

where

h_c average convective heat transfer coefficient

When $T_R > T_A$ (overcast sky), the convective heat transfer is out of the roof and when $T_R < T_A$ (zero cloud cover), the convective heat transfer is into the roof.

Combining equations (1), (2), and (4), the net heat flux becomes

$$Q = \varepsilon\sigma T_R^4 - \varepsilon q_s + h_c(T_R - T_A) \qquad (W/m^2) \tag{5}$$

In this equation the roof temperature, T_R, can be determined using a calibrated aerial scanner as discussed in the following section. Thus, in principle, it is possible to establish the net heat flux, Q, from a flat roof using equation (5) if appropriate values of ε, h_c, q_s and T_A are assigned.

SURFACE TEMPERATURE DETERMINATION FROM SCANNER DATA

The roof surface temperature, T_R, can be determined from remotely sensed thermographic data by relating the scanner measured radiative flux to the surface temperature. In order to obtain temperatures from radiative flux measurements, the aerial scanner used has two adjustable temperature blackbody radiators which serve as high and low temperature reference sources. These reference fluxes (temperatures) and their associated blackbody temperatures are measured and recorded along with the radiative fluxes from surfaces on the ground for each scan line. With the reference fluxes bracketing the terrestrial scene, the scanner is calibrated and an effective radiation temperature, T_{ER}, for each roof surface is determined. This effective temperature is not a true roof surface temperature because: (1) the roof surface is not a blackbody as are the reference sources, and (2) the radiation measured by the scanner (q_{meas}) includes not only the flux emitted ($q_{s\varepsilon}$) by the roof surface but also the flux reflected by the roof ($q_{s\rho}$) from the sky.

The relationship between the remotely measured flux and the flux from the roof surface is:

$$q_{meas} = q_{s\varepsilon} + q_{s\rho}$$

An empirical relationship between the measured fluxes and temperatures is given by reference 4 as:

$$CT_{ER}^5 = C\varepsilon T_R^5 + \rho q_s' = C\varepsilon T_R^5 + (1 - \varepsilon)q_s' \tag{6}$$

where

C proportionality constant = 4.67×10^{-11} $W/m^2\ (K)^5$

= 7.85×10^{-13} $Btu/hr\text{-}ft^2\ (^oR)^5$

ρ roof reflectance = $(1 - \varepsilon)$ for a gray body

q'_s spectral sky flux

The exponent 5 on temperature empirically arises because the scanner system measures the flux in the 8 to 14 μm wavelength region. This wavelength region is used because the atmospheric transmission is high at these wavelengths and also because the radiation from surfaces at temperatures of interest (278 K or 500° R) is a maximum. It should be noted, that because of the finite wavelengths, the spectral sky flux q'_s is not the same as the total or calorimetric sky flux discussed earlier. In order to apply equation (6), an independent value of q'_s is required either analytically or experimentally. For the present study, an experimentally derived value will be used.

EXPERIMENTAL PROCEDURE

Test sites on two building roofs were selected by the GSA for instrumentation. Both buildings were situated so that the background radiation was primarily from the sky. One building has a flat composite roof consisting of a metal deck, insulating material, and built up roofing (tar paper, tar and gravel). This building (Test Site A) was selected because of its high heat loss as shown by a previous thermograph and because it has a flat roof construction that is typical of commercial and industrial buildings. This roof has a thermal resistance, R, value of 0.65 m^2 (K)/W (3.7 hr-ft^2 (°R)/Btu). The second building is of wood frame construction with a pitched roof made of wood sheathing, tar paper, and roll roofing. This building was also selected because of its high heat loss and because it is similar in construction to many residential dwellings. The ceiling for half of this building was uninsulated and half was insulated with 0.25 m (10 in.) of cellulose. The R values were 0.88 m^2 (K)/W (5.0 hr-ft^2 (°R)/Btu) and 7.3 m^2 (K)/W (41.6 hr-ft^2 (°R)/Btu) for the uninsulated half (Test Site B) and insulated half (Test Site C) sections, respectively. A plastic barrier was placed between the two attic sections above the insulated ceilings to minimize air flow between them.

In order to visually locate the test sites easily in the remotely sensed data, aluminum coated panels were placed on the roofs to outline the 3 x 3 m (10 x 10 ft) test sites (fig. 2). Within these test sites, copper-constantan thermocouples were placed on and throughout the roof structures (fig. 3) according to specifications established by both NASA and GSA. During the time of the overflight, roof surface temperatures and temperatures within the structure were measured. A portable emissometer was used to measure the emittances of the roof surfaces which were high and all equal to 0.9. The ambient air temperature and surface wind speed were obtained from the National Weather Service. Neither the calorimetric sky radiation nor the spectral sky radiation were measured. However, methods to calculate these values will be presented in the next section.

The remote thermal data were obtained using a C-47 aircraft and the thermal channel of a commercially available multispectral scanner. The thermal fluxes were digitized and recorded on magnetic tape. The recorded data were then processed at a later date on a ground based minicomputer system (ref. 1). Thermal data were obtained with zero cloud cover between 9:15 p.m. and 9:35 p.m. with an ambient temperature of 272 K (489.6° R and a wind speed of 3.6 m/s (8 mi/hr). The aircraft altitude was 305 m (1000 ft) above the ground with a corresponding ground resolution (pixel) of 0.76 m (2.5 ft) square at nadir. The flight lines were flown so that each test site was near nadir during the time the data were obtained.

EXPERIMENTAL DETERMINATION OF ROOF HEAT FLUXES

A computer printout of the remote digital data recorded for each pixel within the aluminum outline was used to determine the most reliable remotely determined value to compare to the roof surface temperature measured by the thermocouples. A typical profile of the digital data across Test Site A is shown in figure 4. The low digital levels are associated with the aluminum

panels and are due to the low emittance of the aluminum rather than low surface temperature. The important thing to note in figure 4 is that the digital levels (110 to 112) for the roof pixels (6 to 8) within the test site are representative of the roof signal level. In order to verify this, data outside the test site were also examined. Those data also yielded an average value of 112 counts with a variation of ±2 counts in the areas sampled. Thus with this uniformity, 112 counts were used to calculate the roof surface temperature for this test site. This same procedure was used to determine the digital levels for each test site. With the digital levels established for each test site, the effective radiation temperature (T_{ER}) of the roof surface was determined from the scanner calibration procedure discussed previously.

In order to calculate T_R from T_{ER} using equation (6), values for ε and q_s' must be established. The emittance, ε, was measured for each test site, but q_s', the spectral sky flux was not measured directly in this experiment. However, by substituting the measured values of emittance, ε, roof surface temperature, T_R, and scanner effective radiation temperature T_{ER} for Test Site C into equation (6), a value of q_s' of 14.1 W/m^2 (4.5 Btu/hr-ft^2) was found. This value of q_s' was then used to calculate T_R for the remaining two test sites. Test Site C was used to determine q_s' because the building was well isolated meaning that q_s' was primarily controlled by the incoming sky radiation.

With T_R calculated, the roof heat loss, Q, can be determined from equation (5) if the calorimetric sky flux, q_s, and h_c are separately known. Since the experimental data were obtained with zero cloud cover, the calorimetric sky flux was found using a model proposed by Swinbank (ref. 2). This model, which is based on numerous experiments, and therefore should be fairly reliable, gives a calorimetric sky temperature, T_s, as a function of T_A as

$$T_s = 0.0553\, T_A^{1.5} \qquad (T_s, T_A \text{ in K}) \tag{7}$$

so that q_s can be found:

$$q_s = \sigma T_s^4 \tag{8}$$

As noted above, the calorimetric sky flux established in this manner should adequately predict q_s because of the large number of data points used in reference 2. In addition, this sky flux is in substantial agreement with other work (see ref. 3 for example).

On the other hand, assignment of a reliable value for h_c is difficult. Conventionally, a surface conductance is obtained from reference 5 which includes both the convection and radiation portion of the conductance. The radiation portion (4 W/m^2 (K)) can be subtracted from the conductance and an empirical relationship established which gives the convection coefficient as:

$$h_c = 5.39 + 3.65\, v \qquad (\text{W/m}^2\,(\text{K})) \tag{9}$$

where

v wind speed (m/s)

This relationship is based on data from heat transfer between a heated flat plate 0.3 x 0.3 m (1 x 1 ft) and the air. Despite the physical differences between the small plate and a roof, the single value of h_c from equation (9) for each wind speed is then used to represent the average heat transfer coefficient over the entire roof surface. Moreover, Goldstein (ref. 4), has noted that this convective model is not appropriate for several other reasons. The convective coefficient involves both a free convection (5.39) and a forced convection (3.65 v) term. The free convection term in equation (9) is based on data from a heated plate to cooler air where the normal buoyant forces are involved. Therefore it must differ for the clear sky case where the roof is

colder than the air and the buoyant forces are altered.

The forced convection term is also dependent on the air flow length of run from the windward edge of the roof. For this reason, equation (9) is in error since it is based on a length of 0.3 m (1 ft). Thus, each section of the roof has a different convective coefficient associated with it. An estimate for the possible error in the forced convection term can be obtained from reference 4 where the effect of length on h_c was considered. For a length of 0.3 m (1 ft), the results of the calculations presented in reference 4 agreed with equation (9) (ref. 5). However, for longer lengths the effect on h_c was significant. For example, the forced convection coefficient for a length of 5 m is only 72% of that calculated for 1 m. Even with these considerations, the commonly used h_c (ref. 5) obtained from equation (5) will be used to calculate the roof heat loss, Q.

For the present experiment, the most reliable roof heat loss Q can be calculated by using the roof thermal resistance, R, and the inside room temperature, T_{in}, both of which were measured in the experiment. The heat flux from the room air to the roof surface is given by

$$Q = \frac{1}{R}(T_{in} - T_R) \tag{10}$$

This heat flux is also equal to the heat flux between the roof surface and the environment (eq. (5)) so that

$$Q = \frac{1}{R}(T_{in} - T_R) = \varepsilon\sigma T_R^4 - \varepsilon q_s' + (T_R - T_A) \tag{11}$$

Thus, the roof heat loss can be determined in two ways and the results compared.

EXPERIMENTAL RESULTS

The roof surface temperatures measured by the thermocouples and the effective radiation temperature, T_{ER}, determined from the scanner data are shown in Table I along with the remotely determined roof surface temperatures, $T_R(S)$, calculated using T_{ER} in equation (6). The remotely determined roof temperatures, $T_R(S)$, calculated for Sites A and B using q_s' (14.1 W/m^2) determined from Site C agree to within 0.5% (1.2 K) of the thermocouple measured roof temperatures. Since the spectral sky flux q_s' represents an uncertainty in the calculation of the remotely determined roof temperatures, $T_R'(S)$ were also calculated assuming q_s' was zero. These results are also in good agreement (within 1% (2.5 K)) with the thermocouple measurements. Thus, for a high emittance surface (emittance approximately 0.9) on a clear night, the roof surface temperature determined from aerial thermography is estimated to be accurate to within approximately 0.5% when a reasonable value of the spectral sky flux is considered since the sensitivity of the calculation to large changes in q_s' is small.

The roof heat losses obtained using equation (10) [$1/R(T_{in} - T_R)$], with the thermocouple measured roof temperatures, Q(ref), and the remotely determined roof temperatures, Q(S), are shown in Table II. These values of Q agree very closely and are reliable since the R values for the roof structures are known and the effect of small changes in temperature measurements will be minimized since the temperature differences $(T_{in} - T_R)$ are large. As a result, they are the most reliable roof heat flux values and thus will be used as references. In the general case, however, R and T_{in} are not known so that it is necessary to determine Q from equation (5) using the remotely determined roof temperatures and the environmental parameters.

The total heat fluxes along with the radiative ($q_r = \varepsilon\sigma T_R(S)^4 - \varepsilon q_s$) and convective [$q_c = h_c(T_{in} - T_R)$] components calculated using the remotely determined roof temperatures are presented in Table III. A comparison of the total roof heat fluxes calculated in this manner with the reference values shows agreement to better than 17%. However, this agreement may be fortuitous

since, as noted previously, the convective heat transfer coefficient, h_c, is questionable, and the remotely determined temperatures can easily vary by 1 K.

In order to estimate the sensitivity of the total heat flux calculations to small changes in roof surface temperature, the total heat flux, Q, along with its components were calculated for a roof temperature change of 1 K. The results of these calculations are shown in Table III. The small changes in roof temperatures results in significant changes in Q when compared to the reference Q's. In order to see where the small change in temperature has the most significant effect, compare the component terms q_r and q_c in Table III. The radiation components are not significantly affected. However, the convective components differ greatly, indicating the larger sensitivity of this component to small changes in temperature.

In addition, it should be noted that any change in h_c is reflected directly into the convective component. As a result, the determination of total roof heat flux is much more sensitive to the uncertainties in the convective component than those in the radiative component. Consequently, it must be concluded that the use of aerial thermography for quantitative heat loss determination is only feasible when the convective heat transfer can either be determined accurately or its effects minimized.

EFFECTS OF VARIATION IN ENVIRONMENTAL CONDITIONS

Although it appears, as noted above, roof surface heat fluxes cannot be determined with sufficient accuracy because of the convection effects, it is of interest to look at the effects of various environmental conditions upon T_R, Q, and the uncertainty in Q. Hopefully, there are conditions more conducive to an acceptable determination of Q using remote data. Thus, to evaluate this remote possibility, the variation of T_R, Q, and the uncertainty in Q with environmental conditions will be studied using the heat loss model discussed previously.

Surface Temperature and Heat Flux Analysis

The variation of the roof temperature, T_R, with environmental conditions is found by an iterative solution of equation (11) for the different conditions. This value for T_R, is then used in equation (5) to determine the heat loss Q. For this analysis, an uninsulated flat roof, which represents the most interesting case for energy conservation will be considered. An R value of 0.70 m^2 (K)/W (4.0 hr-ft^2 (^oR)/Btu), an inside design temperature of 297.2 K (535.0^o R) (ref. 5), and an emittance of 0.9, which is a typical value for many roof surfaces, was used in the calculations.

The calorimetric sky flux required to make a general study of the effects of environmental conditions, was calculated for both a zero cloud cover and a total cloud cover (overcast). For the zero cloud cover, the calorimetric sky radiation, q_s, was found using equations (7) and (8). For the totally overcast sky, the calorimetric sky flux was determined from the ambient air temperature, T_A (ref. 3) by

$$q_s = \sigma T_A^4 \tag{12}$$

The variation of roof temperature with T_A is shown in figure 5(a) for zero wind speed. The ambient air temperature is also plotted as a reference. For zero cloud cover, T_R, is less than T_A because the net radiation loss $\left(\varepsilon\sigma T_R^4 - \varepsilon q_s\right)$ is large. It should be noted that for this case, the convective heat transfer $[h_c(T_R - T_A)]$ is from the air to the roof so that the roof is gaining heat from the air. For a totally cloud covered sky, T_R, is larger than T_A since the net radiation loss to the sky is much less than for zero cloud cover. In this case, the convective heat transfer is from the roof to the air so that the roof is losing heat to the air.

The effect of the wind speed on roof temperature for a typical ambient temperature of 272.2 K (490.0° R) is shown in figure 5(b). For both cloud conditions, the roof temperature approaches the ambient air temperature as the wind speed increases.

The effect of the environmental conditions on the heat flux, Q, is determined by using the calculated T_R in equation (10). Figure 6(a) shows the variation of Q with ambient temperature for zero wind speed for both sky conditions. In general, the heat loss decreases as the ambient temperature increases. The heat loss for zero cloud cover is greater than that for total cloud cover at all ambient temperatures. Figure 6(b) shows the variation of Q with wind speed for an ambient temperature of 272.2 K (490.0° R). With zero cloud cover, the Q decreases as the wind speed increases since the air is adding heat to the roof. For total cloud cover, the heat loss increases with the wind speed since the roof is losing heat to the air. The effect of wind speed on the magnitude of Q is small in both cases.

In general, it appears that, for both sky conditions, the ambient temperature should be as low as possible making Q as high as possible with any error in Q minimized. No conclusion concerning the effect of wind can be discerned from the variation of T_R and Q with velocity.

Uncertainty Analysis

In order to gain more insight into the environmental conditions that are potentially more favorable for quantitative heat loss determinations using aerial thermography the relative uncertainty in Q will be determined.

The relative uncertainty in heat loss, Q, was found using the procedure given in reference 6. It should be noted that by following this procedure, a maximum uncertainty is found which in all probability is not indicative of the true experimental error. However, for guidance purposes, the trends are the important thing and the analysis should predict these adequately.

Using the procedure of reference 6 and equation (5), the relative uncertainty in Q, $\Delta Q/Q$, is found to be

$$\frac{\Delta Q}{Q} = \left[\left(\frac{\partial Q}{\partial \varepsilon}\frac{\Delta \varepsilon}{Q}\right)^2 + \left(\frac{\partial Q}{\partial T_R}\frac{\Delta T_R}{Q}\right)^2 + \left(\frac{\partial Q}{\partial h_c}\frac{\Delta h_c}{Q}\right)^2 + \left(\frac{\partial Q}{\partial q_s}\frac{\Delta q_s}{Q}\right)^2 + \left(\frac{\partial Q}{\partial T_A}\frac{\Delta T_A}{Q}\right)^2\right]^{1/2} \tag{13}$$

with the individual terms given by

$$\frac{\partial Q}{\partial \varepsilon}\frac{\Delta \varepsilon}{Q} = \frac{\varepsilon\left(\sigma T_R^4 - q_s\right)}{Q}\left(\frac{\Delta \varepsilon}{\varepsilon}\right)$$

$$\frac{\partial Q}{\partial T_R}\frac{\Delta T_R}{Q} = \frac{\left(4\varepsilon\sigma T_R^3 + h_c\right)}{Q}\left(\frac{\Delta T_R}{T_R}\right)$$

$$\frac{\partial Q}{\partial h_c}\frac{\Delta h_c}{Q} = \frac{h_c(T_R - T_A)}{Q}\frac{\Delta h_c}{h_c}$$

$$\frac{\partial Q}{\partial q_s}\frac{\Delta q_s}{Q} = -\frac{\varepsilon q_s}{Q}\left(\frac{\Delta q_s}{q_s}\right)$$

$$\frac{\partial Q}{\partial T_A}\frac{\Delta T_A}{Q} = \frac{h_c T_A}{Q}\left(\frac{\Delta T_A}{T_A}\right)$$

Thus, by using the variations of T_R and Q with environmental conditions presented in figures 5 and 6, the relative uncertainty in Q can be determined. The individual terms in the equation can be determined from the model and reasonable experimental uncertainties except for the relative uncertainty associated with the remote determination of T_R.

The relative uncertainty in T_R, $\Delta T_R/T_R$ determined from equation (6) is:

$$\frac{\Delta T_R}{T_R} = \left[\left(\frac{\partial T_R}{\partial \varepsilon}\frac{\Delta \varepsilon}{T_R}\right)^2 + \left(\frac{\partial T_R}{\partial T_{ER}}\frac{\Delta T_{ER}}{T_R}\right)^2 + \left(\frac{\partial T_R}{\partial q'_s}\frac{\Delta q'_s}{T_R}\right)^2\right]^{1/2} \qquad (14)$$

With the individual terms given by:

$$\frac{\partial T_R}{\partial \varepsilon}\frac{\Delta \varepsilon}{T_R} = \frac{q'_s - \sigma T_{ER}^5}{5\varepsilon\sigma T_R^5}\left(\frac{\Delta \varepsilon}{\varepsilon}\right)$$

$$\frac{\partial T_R}{\partial T_{ER}}\frac{\Delta T_{ER}}{T_R} = \frac{T_{ER}^5}{\varepsilon T_R^5}\left(\frac{\Delta T_{ER}}{T_{ER}}\right)$$

$$\frac{\partial T_R}{\partial q'_s}\frac{\Delta q'_s}{T_R} = \frac{(1-\varepsilon)q'_s}{5\varepsilon\sigma T_R^5}\left(\frac{\Delta q'_s}{q'_s}\right)$$

In the above equations, values for q'_s and the relative error in q'_s, $\Delta q'_s/q'_s$, for both sky conditions are required. For the overcast sky, a generally accepted model exists for q'_s. This model should predict not only a reasonable q'_s but in particular should give a reasonable estimate of $\Delta q'_s/q'_s$ which will also be used for the clear sky case since no model exists here. The single q'_s for clear skies calculated from the experimental data will be used over the ambient temperatures considered. This is a valid approach since references 7 and 8 indicate that q'_s for clear skies does not change greatly with ambient temperature.

With these considerations, the estimated relative uncertainties required to calculate $\Delta Q/Q$ are:

$$\frac{\Delta \varepsilon}{\varepsilon} = 0.02$$

$$\frac{\Delta h_c}{h_c} = 0.10$$

$$\frac{\Delta q_s}{q_s} = 0.01$$

$$\frac{\Delta q'_s}{q'_s} = 0.01$$

$$\frac{\Delta T_A}{T_A} = 0.001$$

$$\frac{\Delta T_{ER}}{T_{ER}} = 0.001$$

For overcast skies, the $\Delta T_R/T_R$ varied between 1.22×10^{-3} and 1.13×10^{-3} over the range of roof temperature associated with the environmental conditions shown in figure 5. With this small variation, a value of 1.2×10^{-3} was used to calculate the $\Delta Q/Q$ for overcast skies. The variation of $\Delta T_R/T_R$ with T_R for zero cloud cover was also found to be small so that a value of $\Delta T_R/T_R$ of 3.2×10^{-3} could be used to determine the variation of $\Delta Q/Q$.

With the $\Delta T_R/T_R$ values established, the variation of $\Delta Q/Q$ with environmental conditions can be calculated from equation (13). Figure 7(a) shows the variation of $\Delta Q/Q$ with ambient temperature. For both sky conditions, data obtained at low ambient temperatures will probably yield the more reliable Q's.

The effect of wind speed on $\Delta Q/Q$ is shown in figure 7(b) for a typical ambient temperature of 272.2 K (490.0° R). For both sky conditions, the $\Delta Q/Q$ increases rapidly with wind speed. Therefore, the remote thermographic temperature data to determine the more reliable values for Q should be obtained with the lowest possible wind speeds. In addition, for all wind speeds, data obtained with overcast skies probably yield the more reliable Q's.

CONCLUDING REMARKS

Aerial infrared data for three instrumented test sites at the Denver Federal Center were obtained in a preliminary study of the feasibility of determining absolute heat losses from building roof tops using aerial thermography. The roof surface temperatures and the heat losses obtained from aerial thermography were compared to those from ground measurements. The results of this experiment indicated that the roof surface temperature can be accurately determined from the scanner data. However, the total roof heat loss cannot be determined with acceptable accuracy because of the large uncertainty in the convective heat transfer component.

The effects of varying the environmental conditions were investigated to see if roof heat losses could be determined with a more acceptable accuracy. The results of this investigation, based upon the currently used heat flux model, indicated that the most reliable quantitative heat loss determination could be obtained under conditions of total cloud cover, low wind speeds and low ambient temperatures.

Although the results of the preliminary feasibility study are inconclusive, they are somewhat encouraging and a more accurate and controlled experiment is required to evaluate the final feasibility of using remotely sensed data for quantitative heat loss determinations. Such an experiment is in progress at NASA Lewis Research Center using an electrically heated thermal test panel with complete instrumentation to measure the surface temperature and the heat flux.

REFERENCES

1. Bowman, R. L.; and Jack, J. R.: Applications of Remote Thermal Scanning to the NASA Energy Conservation Program. NASA TM X-73570, 1977.

2. Swinbank, W. C.: Long-Wave Radiation from Clear Skies. Quart. J. Roy. Meteorol. Soc., Vol. 89, July 1963, pp. 339-348.

3. Bliss, R. W., Jr.: Atmospheric Radiation Near the Surface of the Ground: A Summary for Engineers. Solar Energy, vol. 5, 1961, pp. 103-120.

4. Goldstein, Richard J.: Application of Aerial Infrared Thermography to the Measurement of Building Heat Loss. ASHRAE Trans., Vol. 84, Pt. 1, 1978, Preprint No. 2482.

5. ASHRAE Handbook of Fundamentals. Am. Soc. Heat. Refrig. Air Cond. Eng., 1972.

6. Meyer, Stuart L.: Data Analysis for Scientists and Engineers. John Wiley & Sons, Inc., 1975.

7. Sloan, Raymond W.: The Infrared Emission Spectrum of the Atmosphere. Sci. Rep. 3, Ohio State Univ. Res. Found., 1956. (AFCRC-TN-56-474.)

8. Sloan, Raymond; Shaw, J. H.; and Williams, Dudley: Infrared Emission Spectrum of the Atmosphere. J. Opt. Soc. Am., vol. 45, no. 6, June 1955, pp. 455-460.

TABLE I. - ROOF TEMPERATURES

[Ambient temperature, T_A = 272.0 K; wind speed, v = 3.6 m/s; roof surface emittance, ε = 0.9; sky condition, zero cloud cover.]

Test site	R, m^2 (K)/W	T_{in}, K	T_R(T/C), K	T_{ER}, K	T_R(S), K	T_R^i(S), K
A High heat loss	0.65	306.4	272.0	266.4	270.8	272.1
B High heat loss	0.88	304.4	268.7	265.6	269.9	271.2
C Very low heat loss	7.3	305.1	268.2	268.8	-----	-----

TABLE II. - ROOF HEAT LOSS

$\left[Q = \frac{1}{R}(T_{in} - T_R).\right]$

Test site	R, m^2 (K)/W	T_{in}, K	Q(ref), W/m^2	Q(S), W/m^2
A	0.65	306.4	52	54
B	0.88	304.4	40	39
C	7.3	305.1	1.6	--

TABLE III. - ROOF HEAT LOSS

$\left[Q = q_r + q_c \text{ with: } q_r = \varepsilon\sigma T_R^4 - \varepsilon q_s;\ q_c = h_c(T_R - T_A);\ q_s = 213\ W/m^2;\ h_c = 18.6\ W/m^2\ (K).\right]$

Test site	T_R(S)			T_R(S) + 1 K			Q(ref), W/m^2
	q_r (W/m^2)	q_c (W/m^2)	Q (W/m^2)	q_r (W/m^2)	q_c (W/m^2)	Q (W/m^2)	
A	83	-22	61	87	-4	83	52
B	79	-38	41	83	-21	62	40

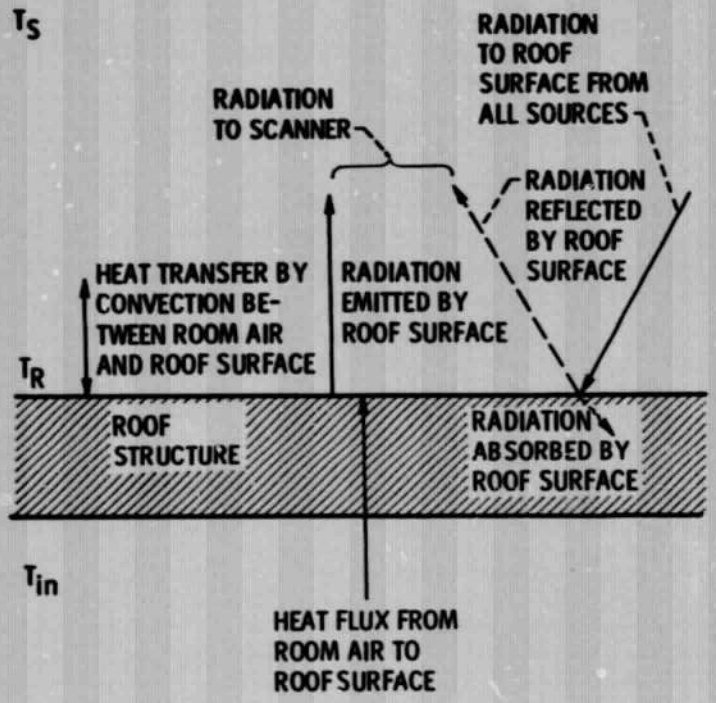

Figure 1. - Heat transfer processes for a flat roof.

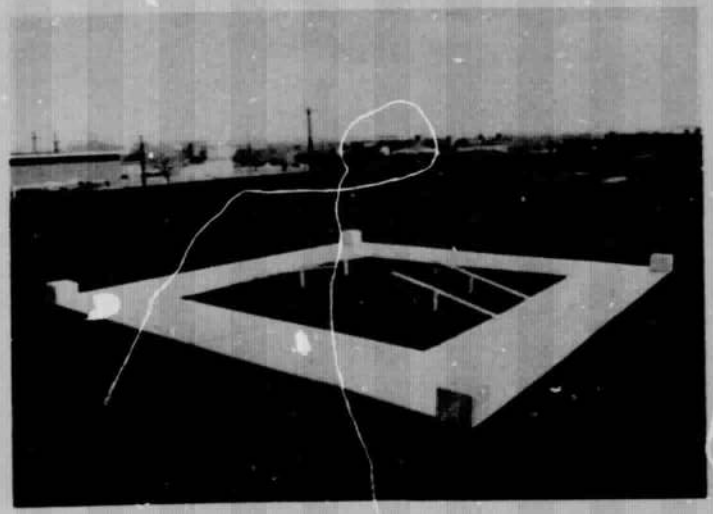

Figure 2. - Instrumented test site A showing aluminum panels at the Denver Federal Center.

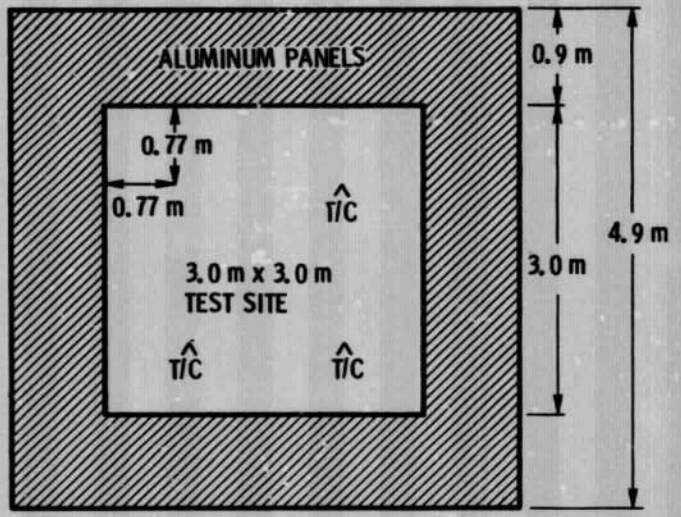

(a) THERMOCOUPLE (T/C) LOCATIONS ON ROOF SURFACE.

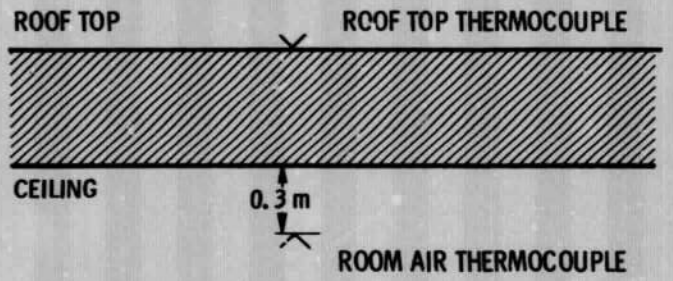

(b) THERMOCOUPLE LOCATIONS THROUGH ROOF STRUCTURE.

Figure 3. - Typical thermocouple locations for instrumented buildings at the Denver Federal Center.

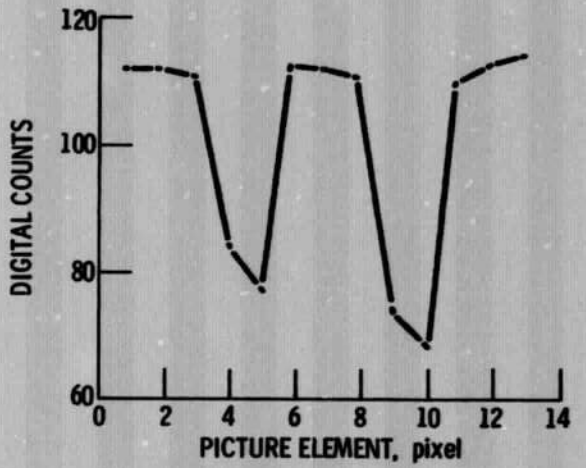

Figure 4. - Scanner signal profile across test site A.

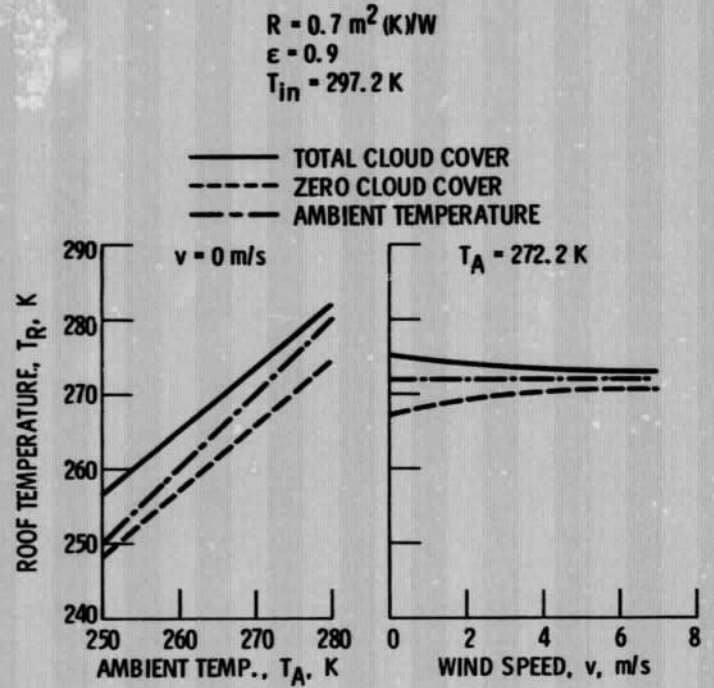

(a) VARIATION OF ROOF TEMPERATURE WITH AMBIENT TEMPERATURE

(b) VARIATION OF ROOF TEMPERATURE WITH WIND SPEED.

Figure 5. - Effect of environmental conditions on roof temperature for a flat roof.

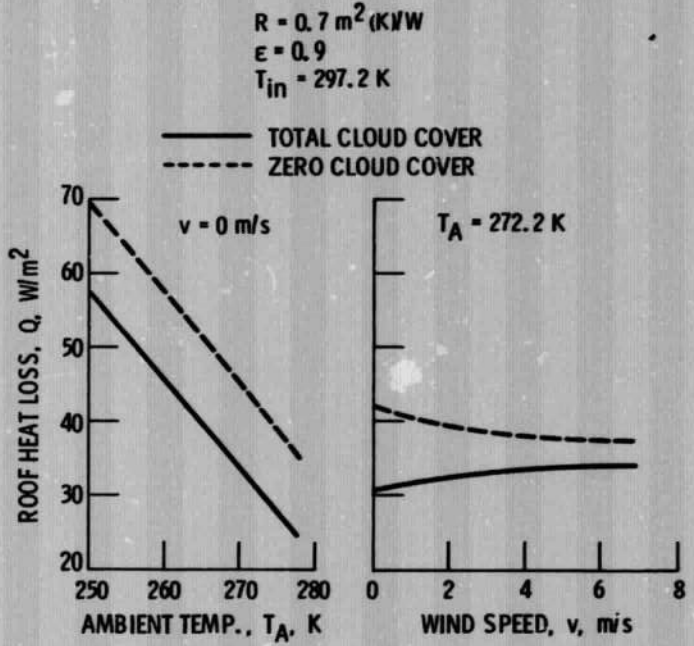

(a) VARIATION IN Q WITH AMBIENT TEMPERATURE.

(b) VARIATION IN Q WITH WIND SPEED.

Figure 6. - Effect of environmental conditions on the heat loss from a flat roof.

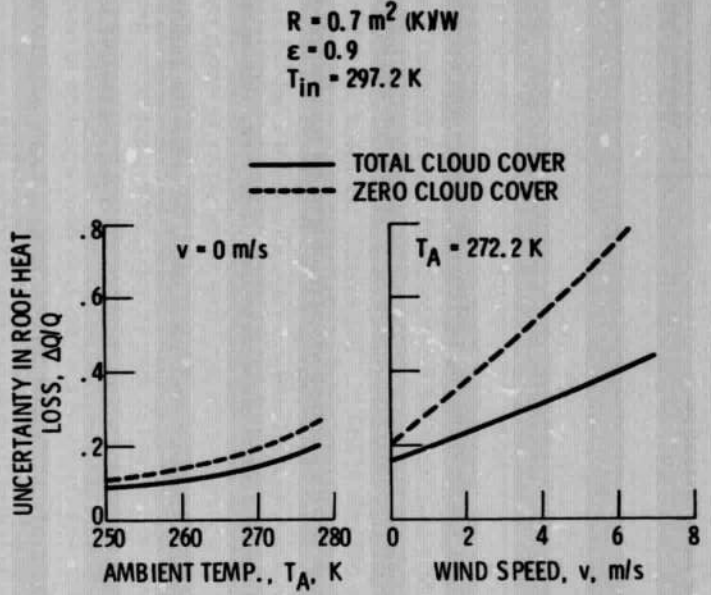

(a) VARIATION OF ΔQ/Q WITH AMBIENT TEMPERATURE.

(b) VARIATION OF ΔQ/Q WITH WIND SPEED.

Figure 7. - Effect of environmental conditions on the relative uncertainly ΔQ/Q for a flat roof.